On the simulation method for producing fine grained HAZ of W strengthened high Cr steel

WANG Xue[a)], XU Qiang[b)], PAN Qian-gang[c)], SHANG Wei[a)], REN Yao-yao [a)], YU Shu-min [a)]

[a] *School of power and mechanics, Wuhan University, Wuhan 430072, China；*

[b] *School of Computing and Engineering, The University of Huddersfield, England*

[c] *DongFang Boiler Group COLTD，Zigong 643001, China*

Version submitted and accepted, its finalized version was published in Materials Science and Engineering: A: Structural Materials: Properties, Microstructure and Processing, 589. pp. 50-56. ISSN 0921-5093

Abstract: Type IV failure, the key life time limiting factor for high Cr steel strengthened with W steel such as P92, occurs in the fine grain heat affected zone (FGHAZ) of a weld. However, the actual size of FGHAZ in a weld is too small (1-2mm), it is necessary to re-produce sizeable uniform specimen for creep tests (such as smooth and notched bar) in order to investigate its creep properties and micro-structural evolutions. This paper investigated two simulation methods for the re-production of FGHAZ, e.g. weld simulator and heat treatment in furnace. The microstructures, hardness, and creep rupture time under 923K/100MPa were investigated and compared with the actual FGHAZ of a weld joint. The dimensional big enough FGHAZ specimen, re-produced by het treatment in furnace, were also crept at 923K/110MPa and 100MPa and compared with that of the base metal. It was found that 1) both the simulated FGHAZ show the similar microstructures and hardness as that of actual FGHAZ of a weld joint, e.g. small grain size (less than 10μm), the disappearance of martensitic lath and the formation of equiaxed grain, and a lowering micro-hardness of 30-40HV , 2) both the simulated FGHAZ demonstrate the similar creep rupture time as that of actual FGHAZ of a weld joint and it is shorter than that of base metal, which is similar to others' finding, 3) in comparison with the base metal, the creep test of FGHAZ reproduced by heat treatment in furnace show a short transitional period and early occurrence of and a prolonged tertiary stage, indicating a deterioration of creep strength. It is concluded that 1) the uniform FGHAZ reproduced via a weld simulator is in the order of 10 to 15 mm long and is not longer enough for creep test; 2) heat treatment in furnace can reproduce the representative FGHAZ required for creep research and the difference of the thermal cycle experienced in a actual welding and heat treatment in furnace is minor and negligible.

Keywords: 9%Cr steel; Heat affected zone; simulation; welded joint; microstructure; creep; Type IV cracking

1. Introduction

New high Cr steels strengthened by replacing Mo with W have been used in ultra super-critical (USC） fossil power plants operating around 873-898K, resulting in considerable reduction of CO_2 emissions [1, 2]. Some of these steels such as ASME P92 steel, have already been put in service in Europe and China [3, 4]. However, the creep strength of a weld of such high creep strength is only as low as 20% of that of the base metal at high temperature and low stress due to cracking in the fine grained heat affected zone (Type IV) [3,4] (7). During the welding process, the base metal, adjacent to the weld material, experienced a different and specific thermal cycle resulting in a newly formed narrow heat affected zone (with width less than 10 mm). It is understood currently that Type IV failure occurs at the fine grain heat affected zone [8,9], which experienced heat peak temperature reaching Ac3 during welding. Currently, though it is generally understood that the Type IV failure is related to the unique microstructure of the FGHAZ (due to the specific thermal cycle) and the mismatch of mechanical properties between the different parts of a weld, it is hardly understand the Type IV failure mechanism.

Hence, it is necessary to conduct a series of investigation on the microstructure evolution during test on thermal aging and creep. Furthermore, it is needed to obtain sizable FGHAZ specimen for the investigation of the influence of states of stress on creep rupture and the typical dimensional size for it is diameter of 5 – 10 mm times length 30 to 100 mm for creep test, diameter of 3- 5 mm with a length of 60 to 100 mm for notched tube creep test, 40 mm by 40 mm for the central square of cruciform test. However, the typical width of FGHAZ in a weld is only 1-2 mm [10-11], not big enough to extract the test specimen directly and simulation method has to be used.

At present, there are two simulation methods, one by heat treatments in furnace and the other by employing a weld simulator. In simulation by heat treatment in furnace, the base metal is heated rapidly in a furnace to the specific peak temperature then after a short duration it is cooled quickly in air [10]. Furnace heating has the advantage that the whole specimen can be heated to the same temperature, and hence, uniform microstructure throughout the specimen. However, the heating and cooling rates that can be achieved are lower than those in an actual weld thermal cycle which may result in a difference of the microstructures between the simulated one and the actual one in weld. A weld simulator can achieve very closely to the heating and cooling rates that experienced by the actual HAZ in the centre of the specimens. Thus, microstructural changes in the HAZ can be more closely simulated. However, due to the current heating method, the uniform heating zone is only 10-15 mm [11, 12], which is not big enough for some of the tests mentioned above.

In this paper, the effeteness of these two simulation methods were investigated by examining microstructures of simulated FGHAZs, micro-hardness test, creep rupture tests at 923K and 100MPa for the two simulated FGHAZs and welded joint to investigate their difference in the rupture life. The creep curve at 923K/ 110MPa and 100MPa of FGHAZ by heat treatment is presented and compared with that of base metal to demonstrate the degradation of creep properties in FGHAZ.

2. Experimental Procedure

2.1. Materials

The material examined was a grade P92 pipe with an outside diameter of 325 mm and a wall thickness of 71mm. Table 1 lists the chemical composition. This pipe was subjected to normalizing at 1343 K for 2 h and tempering at 1053K for 6h. The average grain size of the steel was around 80 μm and the hardness was 240 HV_{98N}. The A_{c1} and A_{c3} temperatures of the steel were 1093 and 1193 K, respectively.

Table 1
Chemical composition of the steel（mass %）

Steel	C	Si	Mn	Cr	Mo	Ni	W	V	Nb	N	B
P92	0.12	0.21	0.43	8.84	0.50	0.16	1.67	0.21	0.067	0.042	0.0033

2.2. FGHAZ simulation by furnace heating

Samples with a diameter of 16.5mm and a length of 190mm were machined out of the pipe parallel to its axis.

They were subjected to the thermal cycle shown in Fig.1a by furnace heat treatment. M.Tabuchi et al. reported that the simulated HAZ specimen of P122 steel heated up to the A_{C3} temperature showed the minimum creep strength [7]. Based on their results, we chose the A_{C3} temperature of P92 steel（1203K）as the peak temperature during heating. From Fig.1a, it can be seen that the heating rate is rapid at the early stage and gradually decreases with time. The material was heated to the peak temperature of 1203K and then cooled in air. Finally, post-weld heat treatment（PWHT）was conducted at 1028K for 5h. Then the simulated samples were machined to the specimens with a gauge diameter of 10mm and a gauge length of 100mm for creep tests to obtain the creep curves, as shown in Fig.1b.

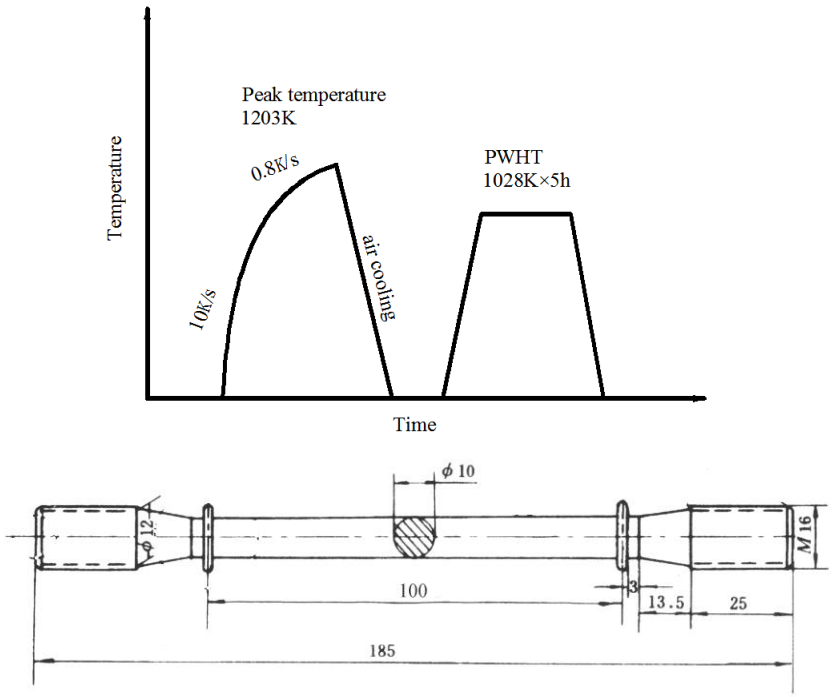

Fig.1 Preparation details of the specimens of FGHAZ simulated by furnace heat treatment. （a）conditions of heat treatment for simulation;（b）creep test specimen

2.3. FGHAZ simulation by weld simulator

The welding thermal cycle shown in Fig.2a was applied by high-frequency induction heating with a THERMECMASTOR-Z simulator. The heating and cooling rates were 80 K/s and 10K/s respectively, and each specimen was held for 3s at the peak temperature of 1203K. The uniform temperature zone corresponding to the simulation temperature at the center of the specimen was found to be about 15～20 mm long， as shown in Fig.2b. After simulation, the specimens were given the same PWHT as those by furnace, and then machined to the size of 10mm in gauge diameter and 50mm in gauge length for creep rupture tests, as shown in Fig.2b.

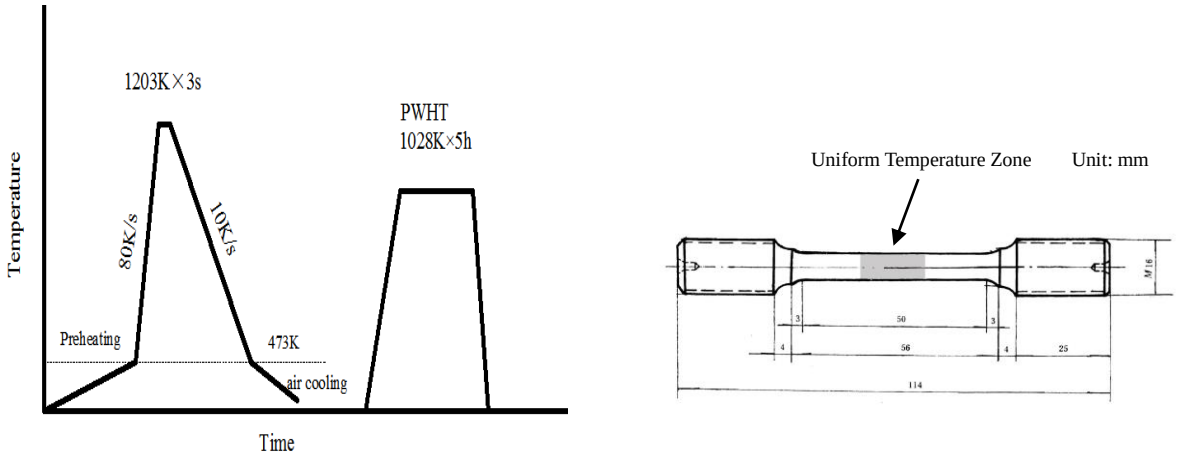

Fig.2 Preparation details of the specimens of FGHAZ simulated by a weld simulator.（a）welding thermal cycle simulation;（b）creep rupture test specimen

2.4. Preparation of welded joints

Welded joints were fabricated from the pipe using submerged arc welding（SAW）with the matching filler metal. The procedure conditions of multilayer SAW are given in Table 2. The same PWHT was conducted on the welded joints. After the PWHT, cross-weld samples with a gauge diameter of 10mm and a gauge length of 80mm were machined out of the welded pipe parallel to its axis. The weld metal was located in the centre of the specimen. To ensure that the real FGHAZ and partial base metal were in the gauge, the gauge length of cross-weld samples were 30 mm longer than those of the simulated FGHAZ specimen by weld simulator.

Table 2
Procedure of welded joint

Groove	U
Wire diameter（mm）	2.4
Welding current（Amp.）	370～390
Arc voltage（Volt）	30～36
Welding speed（m/h）	20～22
Preheating（K）	473-523
Interpass temp.（K）	523-593

2.5. Creep test

Creep rupture tests were performed at 923K and 100MPa on the two simulated FGHAZs and welded joint specimens. Due to the size of FGHAZ produced by weld simulator is too small, only those produced by heat treat in furnace were crept. The creep tests were conducted at 923K/110MPa and 100MPa on the simulated FGHAZ samples by furnace heating and base metal to get the creep curves.

2.6. Microstructural examination and hardness measurement

Microstructural examination was carried out on the specimens of the FGHAZ and base metal before creep

tests using optical and scanning electron microscopes（SEM）. Vilella's reagent was the etchant used to reveal the microstructure. Thin foils prepared from the simulated FGHAZs and base metal were observed by transmission electron microscope（TEM） to investigate their substructures. The hardness values of the simulated FGHAZs, actual FGHAZ in welded joint and base metal were taken with a load of 9.8N for 30s.

3. Results and discussion

3.1. FGHAZ microstructures

Fig. 3 shows the optical micrographs of the two simulated FGHAZ specimens（Fig.3（a）and （b））and the actual FGHAZ （Fig.3（c））near A_{C3} heating of the welded joint after PWHT. The microstructure of base metal in the welded joint was also examined for comparison, as shown in Fig.3（d). There is little difference in OM microstructures between the two simulated FGHAZs and they are approximately the same as the FGHAZ of the welded joint, which has a very fine prior austenite grain size of below 10μm and hence whether the lath microstructure presents or not could not be identified. The base metal has a larger grain size than FGHAZ and consists of the typical lath martensite, as shown in Fig.3 (d).

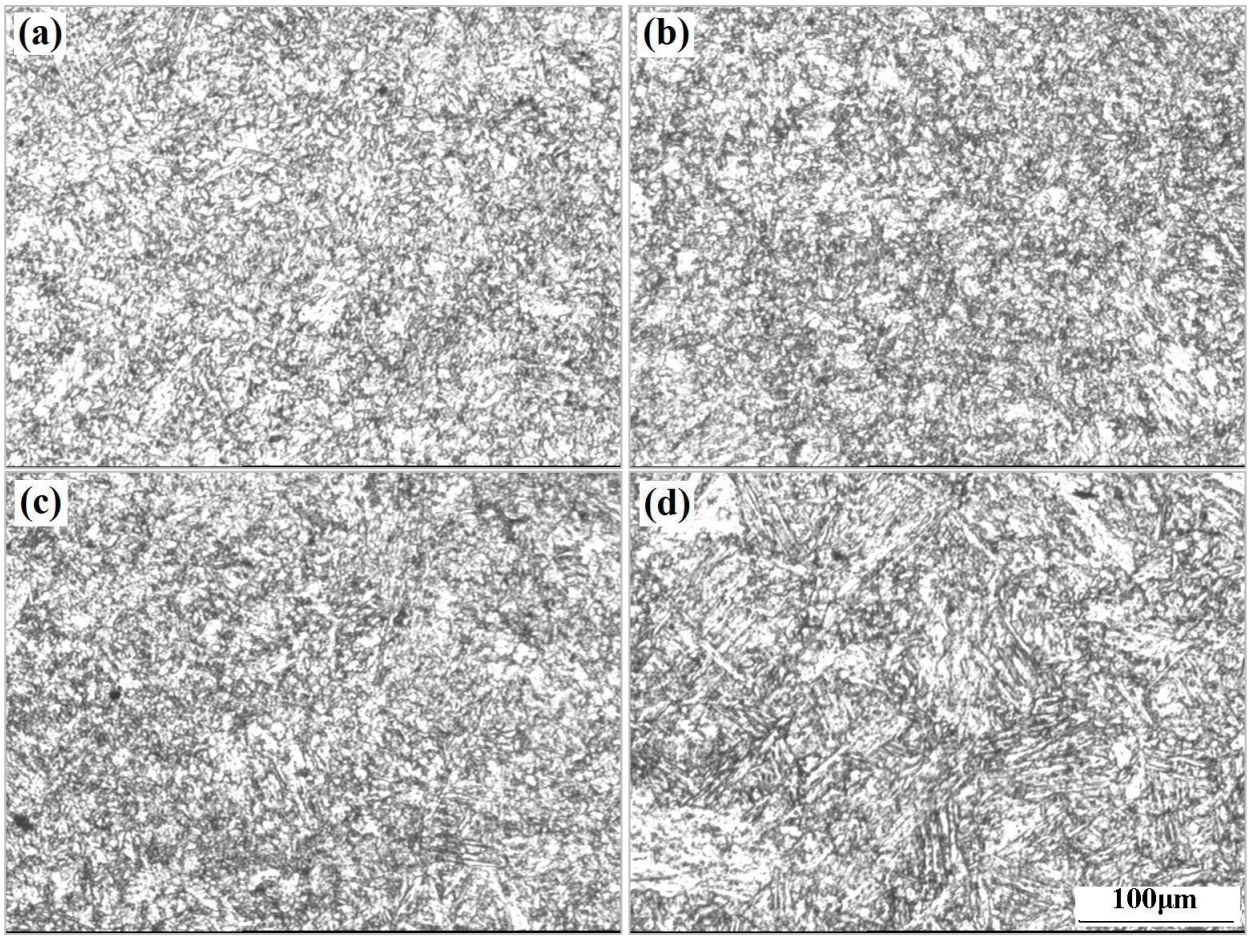

Fig. 3 Optical micrographs of the FGHAZs and base metal after PWHT.（a） simulated FGHAZ by furnace,（b） simulated FGHAZ by weld simulator, （c）real FGHAZ in the weld joint, （d）base metal

Fig. 4 shows the SEM micrographs for the three FGHAZ specimens（Fig.4（a）, （b）and （c））and the

base metal（Fig.4（d））after PWHT. The disappearance of lath structure and the formation of equiaxed grain were observed in both the simulated FGHAZ by furnace and that by weld simulator, which is similar to that in FGHAZ in the welded joint, while the base metal also gives strong evidence of the distribution of thin plates of lath within grain. Two types of precipitates appeared in P92 steel before creep, $M_{23}C_6$ carbide along lath boundaries and MX carbon-nitride in laths [12]. Because MX type precipitate is too small to be observed in SEM micrograph, the precipitates in Fig. 4 can be identified as the $M_{23}C_6$ type carbides. The size and number density of $M_{23}C_6$ carbide are almost the same between the two simulated and the real FGHAZ. Compared with the base metal, the agglomeration and coarsening of $M_{23}C_6$ carbides in the FGHAZ are not obvious. It was reported that $M_{23}C_6$ carbides coarsened remarkably during PWHT and creep in the HAZ of ASME P91 steel （without W ）welded joints[13, 14]. We assumed the addition of W to be a reason for the lower coarsening rate in the FGHAZ of P92 steel, since W could effectively retard the coarsening of $M_{23}C_6$ in 9%Cr maretensite steel [15]. J. Hald et al [16] also reported that the coarsening rate of $M_{23}C_6$ particles in P92 steel was much slower than that in P91 steel during tempering and creep. Although the change of $M_{23}C_6$ particles sizes is small, the difference in the distribution of $M_{23}C_6$ carbides between the FGHAZ and base metal is significant. In the FGHAZ, most coarse $M_{23}C_6$ particles distribute along subgrain boundaries, only a few fine carbide particles can be observed within the subgrains, while $M_{23}C_6$ carbides in base metal are mainly along lath boundaries.

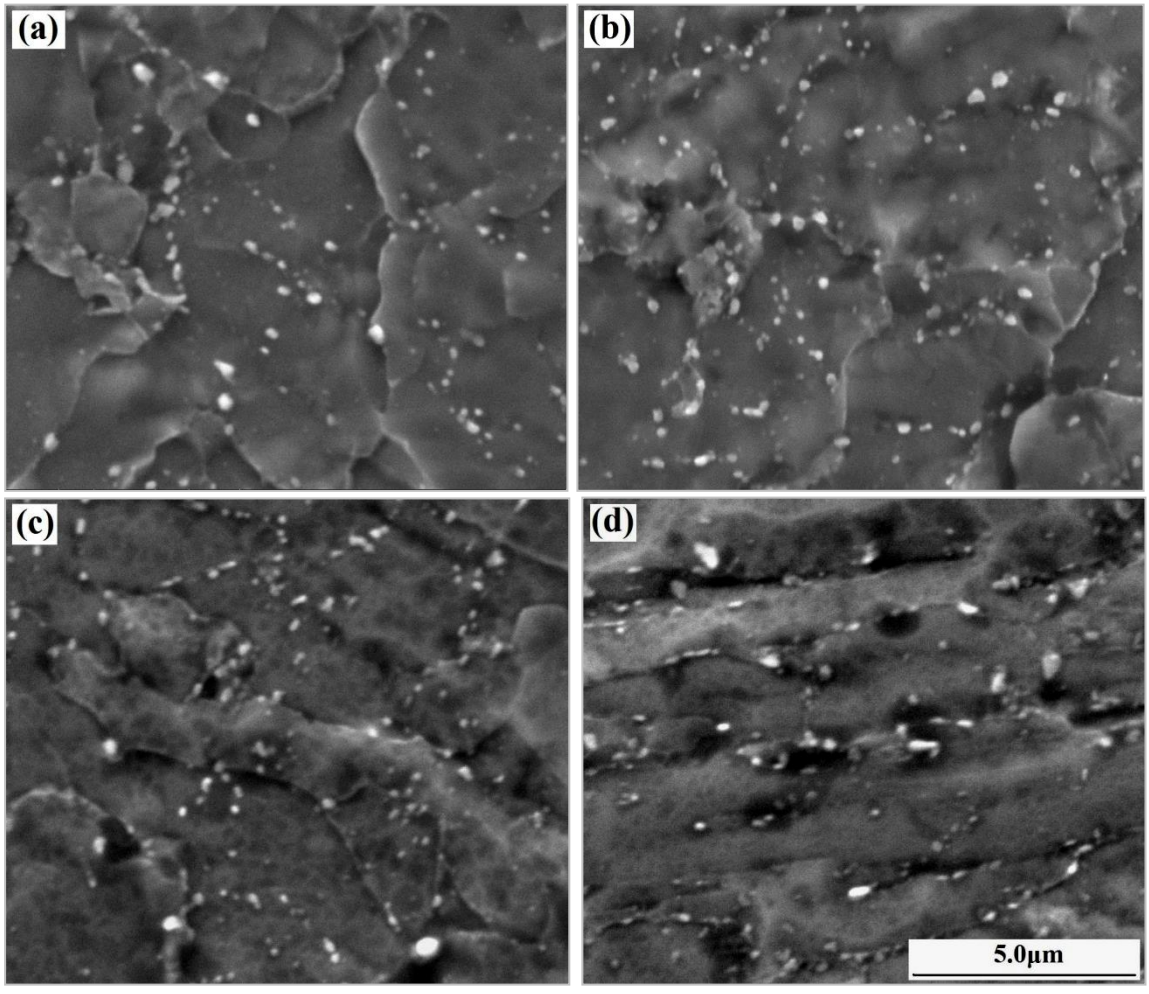

Fig. 4 SEM micrographs of the FGHAZ and base metal after PWHT. （a） simulated FGHAZ by furnace, （b） simulated FGHAZ by weld simulator, （c） FGHAZ in actual weld joint, （d）base metal

According to the above OM and SEM observations, the two simulated FGHAZs show nearly the same microstructures, which are approximately similar to that of real FGHAZ in the welded joint. All of them are much different from that of the base metal.

3.2. FGHAZ substructures

Figure 5 shows the TEM micrographs for the two simulated FGHAZs and the base metal specimens. The real FGHAZ specimen, corresponding to the A_{C3} heating, is difficult to be cut from the welded joint because of its very small width. The two simulated FGHAZs have the similar substructure of coarse subgrains and a low density of dislocations produced by the inhomogeneous recovery during PWHT, similar to the results in the FGHAZ of a P122 steel welded joint reported by Komai N et al [17]. The fine lath substructure was maintained in the base metal and the thin plate of $M_{23}C_6$ carbides distribute mainly along lath boundaries, while the $M_{23}C_6$ carbides in both FGHAZs are globular and distribute mainly along subgrain boundaries, indicating that both of the morphology and distribution of $M_{23}C_6$ carbides changed in the FGHAZs.

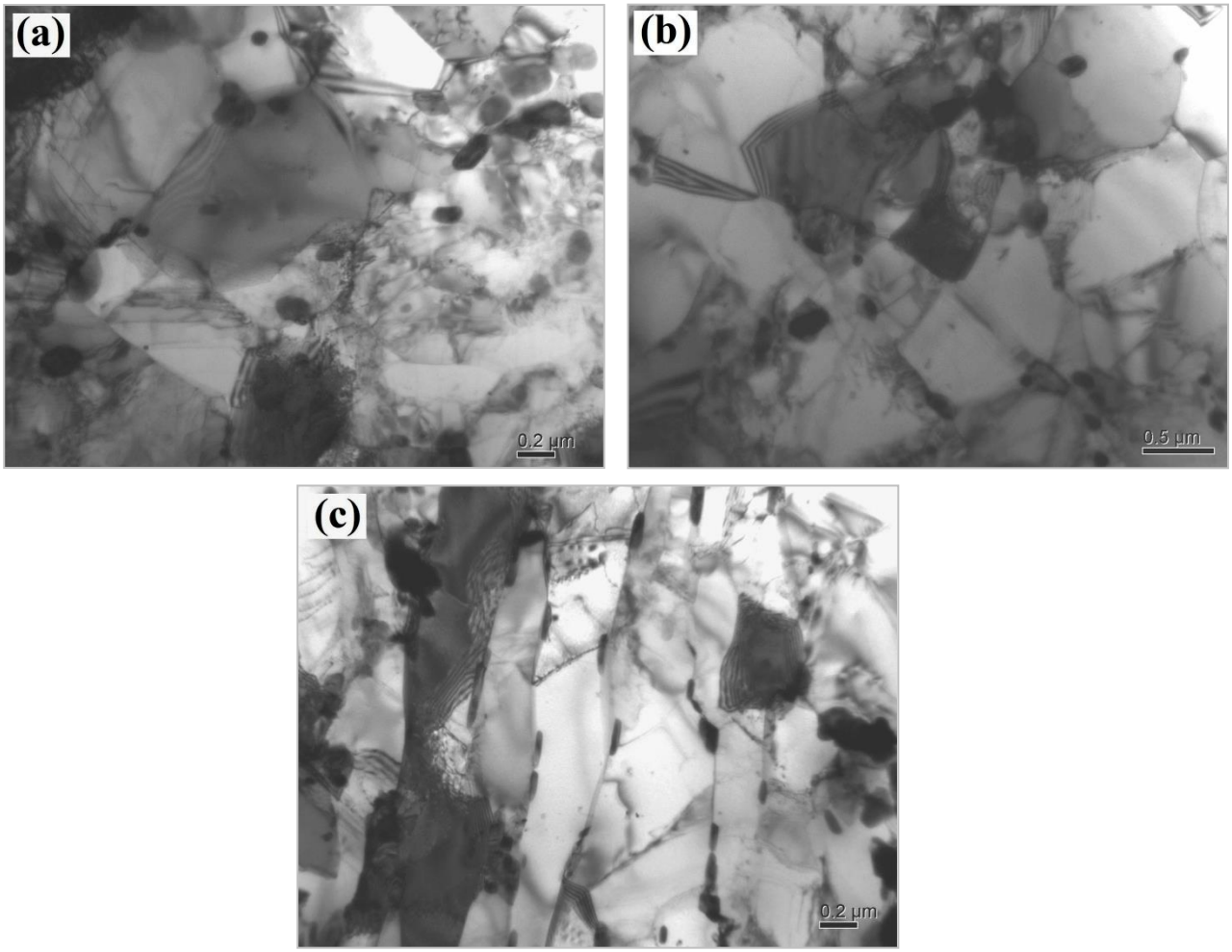

Fig.5 TEM micrographs of the FGHAZs and base metal after PWHT.（a）simulated FGHAZ by furnace,（b）simulated FGHAZ by weld simulator, （c）base metal

From the TEM observations, the substructures for the two simulated FGHAZs are similar and also quite different from that of the base metal.

3.3. FGHAZ microhardness

Fig.6 shows the microhardness of the three FGHAZs alongside with that of base metal. The simulated FGHAZ by furnace heating has the hardness of HV203 and exhibits almost the same minimum as the FGHAZ corresponding to the A_{C3} heating in the welded joint. The hardness of the simulated FGHAZ by welding simulator is slightly higher than that of the simulated FGHAZ by furnace, but about 30HV lower than that of the base metal. The results of the hardness indicate that softening occurred in the FGHAZ after PWHT, and it was caused by the preferential recovery around prior austenite grain boundaries, which produced the coarse subgrains and the low density of dislocations, as shown in Fig.5. The similar reduction in the hardness was observed in the FGHAZ corresponding to a peak temperature close to A_{C3} in P122 steel welded joints [10,17].

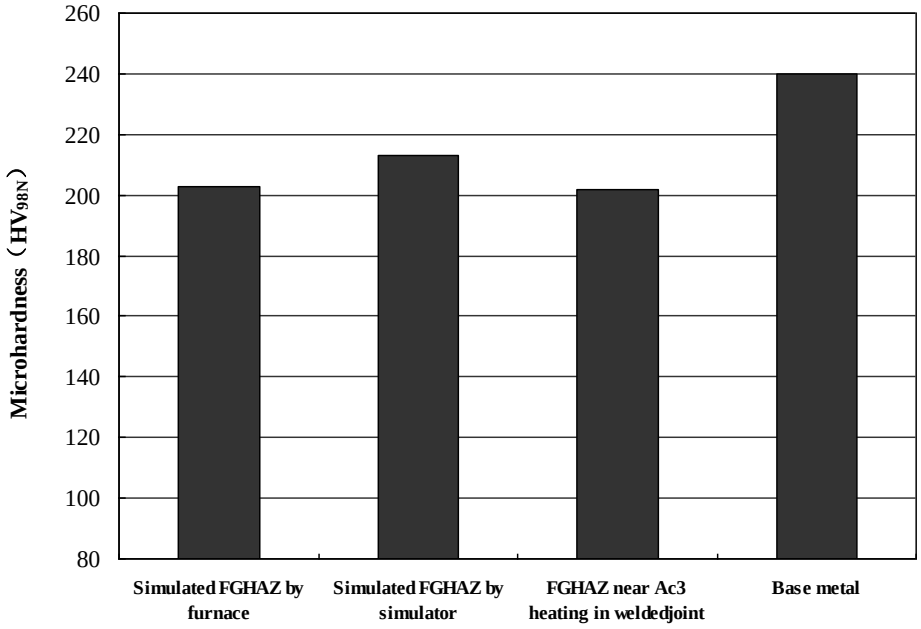

Fig.6 Microhardness of the three FGHAZs and the base metal after PWHT

3.4. FGHAZ creep properties

Fig.7 shows the creep rupture times of the two simulated FGHAZs alongside with the creep rupture times for welded joint and base metal for reference, at 923K/100MPa. First, the creep rupture times show nearly the same value of around 800 h for the two simulated FGHAZs. Second, both are much shorter than that of the base metal indicating a much FGHAZ is much weaker region.Thirdly, the creep rupture life is also shorter than the welded joint (suffering the Type Iv failure). This is not the main concern of current research and the short explanation for this is the multi-axial states of stress induced by the mismatch of creep properties among the different regions of a welded joint.

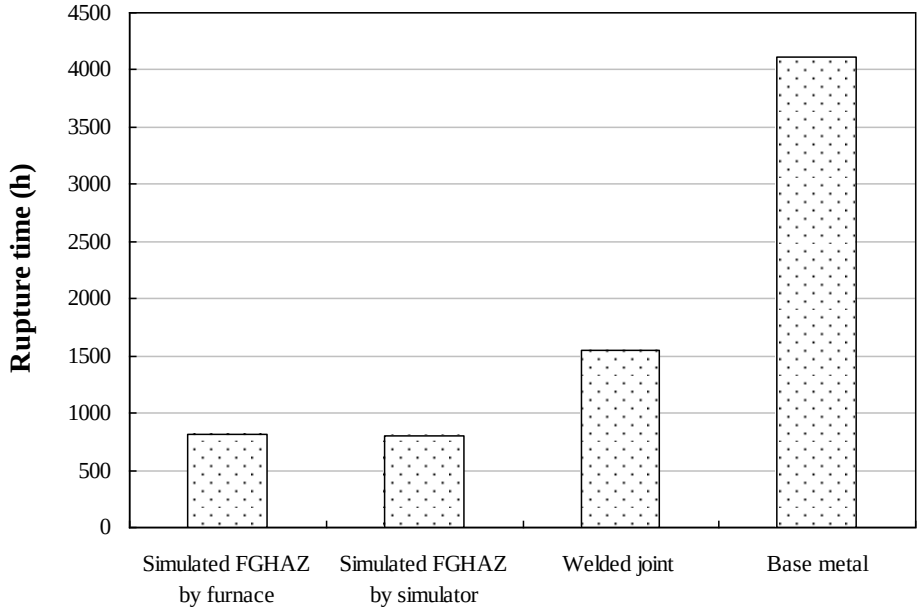

Fig.7 The creep rupture times of the two simulated FGHAZs and the welded joint at 923K/100MPa

Fig.8 shows the appearance of the ruptured specimens of two simulated FGHAZ alongside with that of welded joint. It is clear that both showing similar degree of necking. The rupture of welded joint is complicated by the multi-axial state of stress and test of such specimen is not really giving precise information and further emphasize the need to investigate the properties of the individual regions, particularly the weakest fine grained HAZ.

Fig.8 Appearances of creep rupture specimens for（a） simulated FGHAZ by weld simulator, （b）welded joint and （c）simulated FGHAZ by furnace

We have already reported that the weldment of P92 steel exhibited Type Ⅳ failure in the FGHAZ heated to just above A_{C3} temperature at 923K/100MPa [9]. From the above observations, the simulated and real FGHAZs heating to the A_{C3} temperature have almost the same microstructure, but the later have a longer rupture life and lower ductility. These differences in creep rupture behaviour between them are caused by the multiaxial stress state introduced into the real FGHAZ due to the significant heterogeneity of creep properties in the weld joint [18,

19]. The FGHAZ of nearly A_{C3} heating have the lowest creep resistance among the different zones of the welded joint and its width was less than 1mm. Therefore, its deformation during creep is prevented by the mechanical constraint of the base metal on one side and the coarse grained heat affected zone (CGHAZ) and weld metal on the other side, producing multiaxial stress state in this area. The multiaxial stress state in the weld joint has two effects. First, it suppresses deformation and thus has a strengthening effect, accordingly, the onset of the tertiary creep would be delayed and the rupture life would be longer. Second, it promotes the nucleation and growth of creep voids, resulting in the fracture lack of ductility. Figure 9 shows the microstructures of the welded specimen after 1546.3h and simulated FGHAZ specimen after 810h at 923K/100MPa. Many voids were observed in the FGHAZ of welded joint, no creep voids occurred in the simulated FGHAZ specimen and its grains were much enlongated. This means that the multiaxial stress is a main reason for the creep voids and reduction of the ductility in a weld joint.

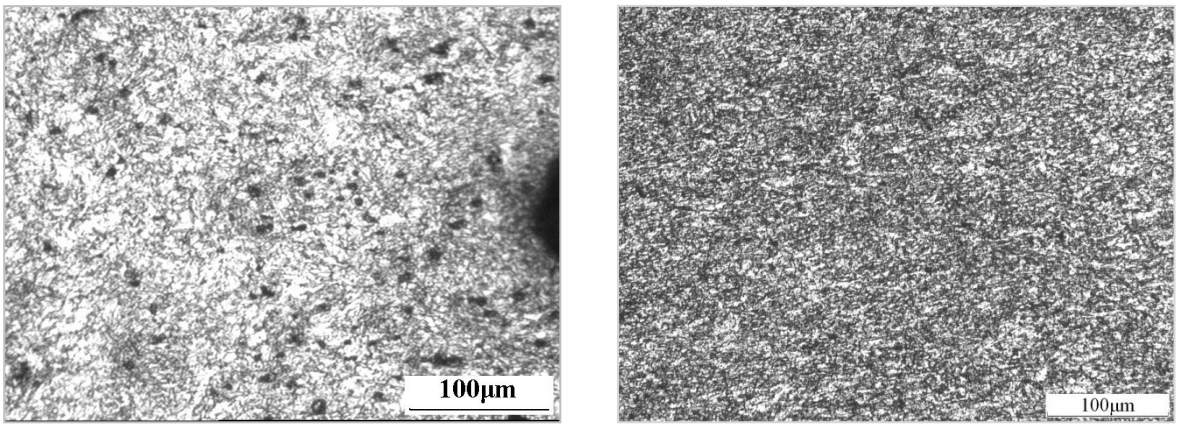

Fig. 9 Optical micrographs of the creep fractured specimen at 923K/100MPa. （a）FGHAZ in a weld joint,（b）simulated FGHAZ

The variation of creep strain with time at 923K/110MPa and 100MPa for the simulated FGHAZ by furnace is shown in Fig.10, where the corresponding variation for the base metal is also shown for comparison. It can be seen that creep strain and the steady creep rate for the simulated FGHAZ are considerably higher than those of the base metal. The simulated FGHAZ specimen exhibits a shorter duration of the transient creep and enters into the tertiary creep-more rapidly and hence obtains a shorter time to rupture compared with the base metal, suggesting that its creep properties deteriorated markedly. The change of microstructure observed in the FGHAZ, the disappearance of lath structure and the formation of coarse equiaxed substructure may be the main reason for the drop of creep strength. Moreover, we believe that the change of distribution of $M_{23}C_6$ carbides in the FGHAZ during PWHT may be also a reason for the degradation of creep strength.

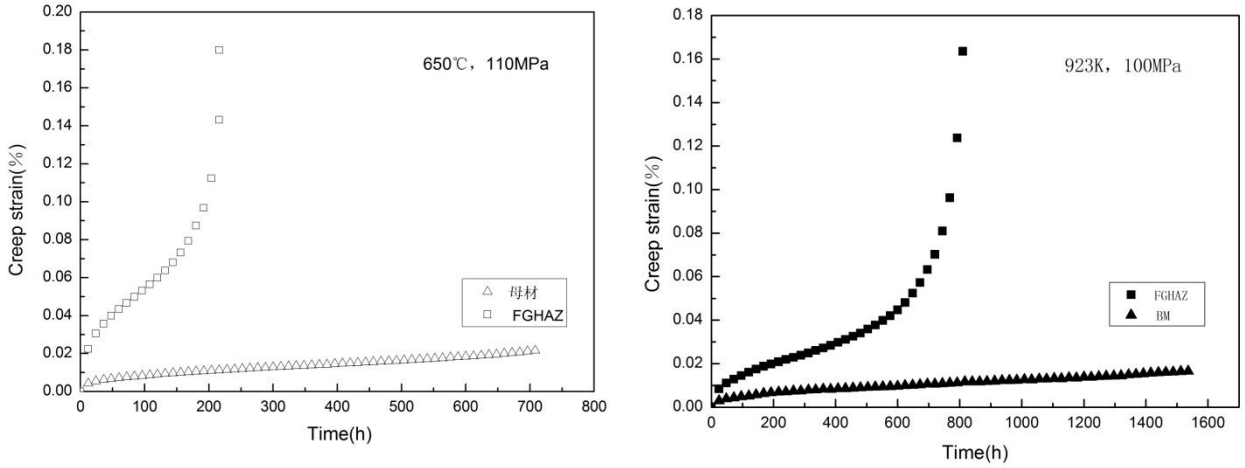

Fig.10 Creep curves of the simulated FGHAZ and the base metal at 923K/110MPa（a）and 100MPa（b）

4. Conclusions

In order to re-produce the FGHAZ with the sizeable dimension and appropriate microstructures and creep properties, two simulation methods (simulation by furnace heat treat meant and welder simulator) were investigated. The main conclusions are:

1. It was found both can re-produce the required microstructures and showing the expected creep properties, however, it seems that the simulator method is limited, to certain degree, to the length of specimen.

2. The two simulation methods can re-produce the required microstructure: a very fine grain size of below 10μm and the substructure without lath structure and formation of equiaxed subgrain.

3. The two simulation methods can re-produce the similar microhardness. The slight difference in micro-hardness between the two simulated FGHAZs and the actual FGHAZ can be further traced/improved based more accurate understanding of the dependence of Ac3 on the heating rate. This is of minor in this paper.

4. The simulated FGHAZ by heat treatment has a shorter duration of the transient creep and rapider onset of tertiary regime and hence the shorter time to rupture compared with the base metal, suggesting that its creep properties deteriorated markedly.

5. Creep rupture times of the two simulated FGHAZs at 923K/100MPa are nearly the same , and they are shorter than that of the welded joint exhibited Type Ⅳ failure as expected. This further requires the research and understanding the individual regions of a weld joint as others have expressed similarly.

6. In order to speed up the creep test, a higher temperature was used. As the creep deformation and damage evolution (either due to the microstructural stability or the cavitation) may is different temperature and stress level, the two perceived similar microstructures reproduced by simulation may behavior differently for a long term low stress test but this is the best we can do scientifically at this moment.

References

[1] Masuyama F. New development in steels for power generation boilers. In: Viswanathan R, Nutting J, editors. Advanced heat resistant steels for power generation. London: IOM Communications Ltd; 2002. p. 33-46.

[2] Bakker WT, Nath B. Development and testing of ferritic steels for advanced power plants: program overview. In: Viswanathan R, Bakker WT, Parker JD, editors. Proceedings of the Third Conference on advances in Materials Technology for Fossil Power Plants. London: The Institute of Metals; 2001. p. 3-6.

[3] Bendic W, Deshayes F, Haarmann K, Vaillant JC. New 9-12% Cr steels in boiler tubes and pipes: operating experiences and future developments. In: Viswanathan R, Nutting J, editors. Advanced heat resistant steels for power generation. London: IOM Communications Ltd; 1999. p. 133-43.

[4] SHEN Qi, LIU Hong-guo. Application of new type heat-resistant steel T/P92 and T/P122 in ultra-supercritical unit and quality control. Electric Power Construction 2010; 31(10): 71-5.

[5] Kern T.-U, Staubli M, Scarlin B. The European efforts in material development for 650℃ USC power plants—COST522. ISIJ Int 2002; 42(12):1515-9.

[6] Abe F, Okada H, Wnanikawa S,Tabuchi M, Itagaki T, Kimura K, Yamaguchi K, Igarashi M. Guiding principles for development of advanced ferritic for 650℃ USC boilers: In: Lecoute-Beckers J, Carton M, Schubert F, Ennis PJ, editors. Proc. of Seventh Liege Conference on Materials for Advanced Power Engineering, 2002. Forschungszentrum Julich 2002;650:1397-406.

[7] Tabuchi M, Watanabe T, Kubo K, Matsui M, Kinugawa J, Abe F. Creep crack growth behavior in the HAZ of the weldments of W containing high Cr steel. Int J pressure Vessel Piping 2001;78:779-84.

[8] Hasegawa Y, Ohgami M, Okumara Y. Quantification of the factors for Type Ⅳ softening of tungsten containing creep resistant steel ASME Gr.92'. In Viswanathan R, Bakker WT, Parker JD, editors. Proceedings of the Third Conference on advances in Materials Technology for Fossil Power Plants. London: The Institute of Metals; 2001. p. 457-66.

[9] WANG Xue, PAN Qian-gang, LIU Zhi-jun, ZENG Hui-qiang, TAO Yong-shun. Creep rupture behavior of P92 steel weldment. Engineering Failure Analysis; 2001;18:186-91.

[10] Albert SK, Matsui M, Watanabe T, Hongo H, Kubo K, Tabuchi M. Microstuctural investigation on Type Ⅳ cracking in a high Cr steel. ISIJ Int 2002;42（12）:1497-504.

[11] Albert SK, Matsui M, Hongo H, Watanabe T, Kubo K, Tabuchi M. Creep rupture properties of HAZs of a high Cr steel simulated by a weld simulator. Int J pressure Vessel Piping 2004;81:221-34.

[12] Abe F. Precipitate design for creep strengthening of 9% Cr tempered martensitic steel for ultra-supercritical power plants. Sci Technol Adv Mater 2008;9 013002:1-15.

[13] Gaffard V, Gourgues-Lorenzon A F, Besson J. High temperature creep flow and damage properties of the weakest area of 9Cr1Mo-NbV martensitic steel weldments. ISIJ Int 2005;45（12）:1915-24.

[14]Abd El-Azim M E, Nasreldin A M, Zies G, Klenk A. Microstructural instability of a welded joint in P91steel during creep at 600℃. Mater Sci and Technol 2005;21（7）:779-90.

[15]T.Hasegawa, Y.R.Abe, Y.Tomita, N.Maruyama, M.Sugiyama. Microstructural evolution during creep test in 9Cr-2W-V-Ta steels and 9Cr-1 Mo-V-Nb steels. ISIJ Int2001 ; 41（8）: 922-929.

[16] Y.J.Hald, L.Korcakova. Precipitate stability in creep resistant ferritic steels experimental investigations and modelling. ISIJ Int 2003; 43（3）: 420-427.

[17]Komai N, Masuyama F. MIcrostructural degradation of the HAZ in 11Cr-0.4Mo-2W-V-Nb-Cu steel（P122）during creep. ISIJ Int 2002;42（12）:1364-70.

[18] Albert SK, Tabuchi M, Hongo H, Watanabe T, Kubo K, Matsui M. Effect of welding process and groove angle on type Ⅳ cracking behavior of weld joints of a ferritic steel. Sci Technol Welding Joining2002;10（2）:149-57.

[19] Albert SK, Matsui M, Watanabe T, Hongo H, Kubo K, Tabuchi M. Variation in the Type Ⅳ cracking behavior of a high Cr steel weld with post weld heat treatment. Int J pressure Vessel Piping 2003;80:405-13.

Acknowledgements

The author would like to express their gratitude for projects supported by the National Natural Science Foundation of China (51074113) and the Fundamental Research Funds for the Central Universities（115005）.